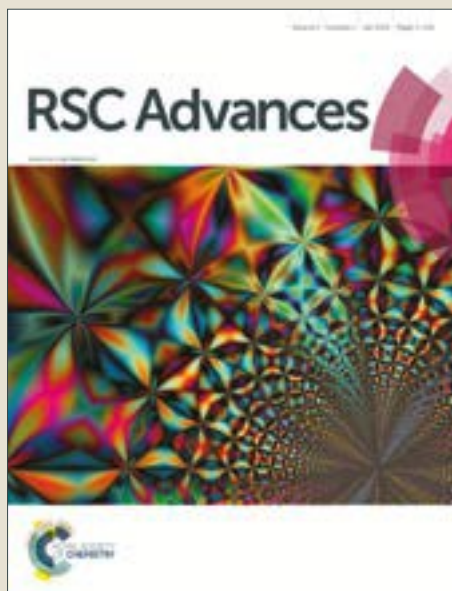


RSC Advances

Accepted Manuscript



This article can be cited before page numbers have been issued, to do this please use: B. Inturi, G. V. Pujar, V. B. Iyer, P. Madhusudan N, S. GS and M. Kulkarni, *RSC Adv.*, 2016, DOI: 10.1039/C6RA19821J.



This is an Accepted Manuscript, which has been through the Royal Society of Chemistry peer review process and has been accepted for publication.

Accepted Manuscripts are published online shortly after acceptance, before technical editing, formatting and proof reading. Using this free service, authors can make their results available to the community, in citable form, before we publish the edited article. We will replace this Accepted Manuscript with the edited and formatted Advance Article as soon as it is available.

You can find more information about Accepted Manuscripts in the [author guidelines](#).

Please note that technical editing may introduce minor changes to the text and/or graphics, which may alter content. The journal's standard [Terms & Conditions](#) and the ethical guidelines, outlined in our [author and reviewer resource centre](#), still apply. In no event shall the Royal Society of Chemistry be held responsible for any errors or omissions in this Accepted Manuscript or any consequences arising from the use of any information it contains.

Design, synthesis and evaluation of diphenyl ether analogues as antitubercular agents

Bharathkumar Inturi¹, Gurubasavaraj V Pujar^{1*}, Madhusudhan N. Purohit¹, Viswanathan B.Iyer¹,
Sowmya G.S² and Madhuri Kulkarni²

¹Department of Pharmaceutical Chemistry, JSS College of Pharmacy, Jagadguru Sri Shivarathreeshwara University, Mysore-570015, Karnataka, India.

²Department of Microbiology, JSS Medical College and Hospital, Jagadguru Sri Shivarathreeshwara University, Mysore-570015, Karnataka, India.

***Corresponding author:**

Dr. Gurubasavaraj V. Pujar, Professor, Department of Pharmaceutical Chemistry, JSS College of Pharmacy, Jagadguru Sri Shivarathreeshwara University, Mysore 570015, Karnataka, India,
Email: gvpujar@jssuni.edu.in, Phone: +918088532266; Fax: +918212548359

ABSTRACT

We here report the investigation of new diphenyl ethers as *Mycobacterium tuberculosis* enoyl-acyl carrier protein reductase (InhA) inhibitors by structure-based drug design approach. The virtual library of diphenyl ethers was designed and molecules with appreciable physicochemical and ADMET properties were docked. The best ranked molecules based on docking studies were synthesized and characterized by spectral studies. Synthesized compounds were evaluated for *in vitro* antitubercular activity against *Mycobacterium tuberculosis* H₃₇R_v strain by Microplate Alamar Blue Assay. Among the tested compounds, **DE3** and **DE2** exhibited substantial antitubercular potential at 3.125 and 6.25 µg/mL concentrations respectively. The most active compounds were further evaluated for cytotoxicity studies against Vero and HepG2 normal cell lines by Microculture Tetrazolium assay and, ascertained to be safe against normal cell. The molecular dynamic study reveals that the best active compounds have shown better binding free energy than the reference compounds TCI and JPL at *Mtb* InhA binding site.

Keywords: Diphenyl ethers; Docking; InhA; Molecular Dynamics; *Mycobacterium tuberculosis*; Triclosan.

1. Introduction

Mycobacterium tuberculosis (*Mtb*) infection has been marked for mortality over two million people worldwide every year. The World Health Organization reports indicated that at the end of year 2020¹ more than one billion populations worldwide may be infected with tuberculosis (TB). Clinical studies indicate that TB is more prevalent susceptible in AIDS patients and, there is an increase in TB epidemics over the last five years may be associated to HIV co-infection. The current status of tuberculosis is magnified due to increase in multidrug resistant to the existing drug therapy²⁻⁴.

Currently, the three major challenges that hinders our ability to eradicate TB effectively are drug resistance strain infection, HIV co-infection and regimen non-compliance. Consequently, there is a need of addressing the issues of multidrug resistance and persistent TB infection. In view of these facts, the development of drugs with novel modes of action has been the crucial of the investigators. The pursuit for inhibitors targeting enzymes that are deemed specific, essential for the replication and persistence of *Mtb* has been the core of antitubercular research. The target-based screening approach for the discovery of new drugs was rendered possible with the advances in proteomics, genomics and molecular genetics of mycobacterium. The target-based screening approach yielded remarkable results in the field of cancer drug discovery and hope that the same would results for TB drug discovery too.

The mycobacterial fatty acid synthase I (FAS I) and FAS II contributes in the biosynthesis of mycolic acids, which are components of the mycobacterial cell wall. Whilst, FAS II has a predominant role in the elongation of fatty acids derived from the end product of FAS I⁵. The terminal step of FAS II, trans-enoyl reduction is catalyzed by InhA and is marked for this significant role. InhA catalyze the elongation of C16 fatty acid and longer, which is different from Enoyl -ACP reductase (ENR) of other bacterial species. InhA has been validated as a promising target for antitubercular drug discovery. Isoniazid (INH) and ethionamide (ETH) the first line agents, and most prescribed drug to treat tuberculosis (TB), inhibits a NADH-dependent InhA that provides precursors of mycolic acids. They are pro-drug that needs activation to form the inhibitory INH/ETH-NAD adduct by KatG/ EthA encoding enzyme. These adducts are marked as tight binding inhibitors of *Mtb* InhA^{6,7}. The mutations of KatG and EthA have been identified and are associated with the development of *Mtb* resistance to the INH and ETH, respectively^{8,9}. The inhibitors which can directly inhibit InhA without activation by KatG/ EthA

can able to circumvent INH/ETH resistance mechanism. This approach is useful in the rational design of potential antitubercular agents against MDR-TB and XDR-TB strains.

The pursuit for small molecules as potential *Mtb* InhA inhibitors is an effective strategy to eradicate MDR-TB. Clinical studies highlight the importance of direct InhA inhibitors and investigation of new small molecules for the same is on worldwide. The new small molecules like pyrazoles¹⁰, indole-5-amides¹¹, diphenyl ethers^{12,13}, pyrrolidine carboxamides¹⁴, arylamides¹⁵, imidazopiperidines¹⁶ and 4-hydroxy-2-pyridones¹⁷ have been reported as direct InhA inhibitors. These molecules can inhibit InhA without prior activation by KatG and have shown potential activity against MDR/INH-resistant TB strains. The Triclosan (TCl), a diphenyl ether derivative was found to be a potent inhibitor of *Mtb* InhA with K_i value of 0.22 mM and MIC value 12.5 $\mu\text{g}/\text{mL}$ ¹⁸. However, TCl use as antitubercular agent is limited due to its poor bioavailability. The biochemistry involved in bacterial inhibition of TCl with the InhA is possible through the π - π ring stacking interactions between the aromatic ring of TCl and pyridine of NAD^+ cofactor. TCl also exhibits strong hydrogen bonding with Tyr 158 residue at the catalytic site and NAD^+ cofactor¹⁹.

In order to improve the bioavailability, TCl modified derivatives were synthesized with improved pharmacokinetic parameters in the last decade, and these new compounds have shown significant activity against both susceptible and resistant *Mtb* strains. In continuation and exploring the structure-activity relationship (SAR), the alkyl substituted diphenyl ethers were synthesized with an improved affinity towards InhA inhibition. In this regard, 5-octyl-2-phenoxyphenol has shown a potential activity (MIC:6-9 μM) against both drug-sensitive and drug resistant strains of *Mtb* and, more importantly the mechanism of inhibition of InhA is KatG independent⁵. The SAR highlights the InhA inhibitory potency also depends on the length of the alkyl chain at 4th position of the A-ring. The optimal activity was observed with alkyl chain length between 3-5 carbons. The removal of the two chlorine atoms on the diphenyl ether B-ring moiety and also replacement of the chlorine function with an ethyl group in A-ring resulted in a 2-fold increase in the IC_{50} value in comparison to TCl (**Figure-1**). In spite of these structural modifications in improvising the antitubercular efficiency, the limited bioavailability was the foremost drawback of these alkyl chain substituted diphenyl ether derivatives may be attributed to the higher log P values (>5). Hence, the investigation was focused to develop druggable diphenyl ethers with improved antitubercular activity with appreciable ADMET properties using

structure-based drug design approach. We report herein the molecular docking, synthesis, antimycobacterial evaluation and molecular dynamics study of new diphenyl ether derivatives.

2. Results and Discussion

2.1. Strategies of drug design

In view of facts discussed earlier, the present work was aimed to develop diphenyl ethers with the optimal lipophilicity (log P values between 3 and 5) as favorable for drug likeness properties. Prior to the drug design strategy, the reported diphenyl ethers physicochemical properties were studied. The results highlights that most of the compounds have significantly higher log P values (>5), while other physicochemical parameters were well within the acceptable range. These compounds have exhibited potent *in vitro* antitubercular activity and their Clog P values ranged between 4 and 7. Despite their promising *in vitro* activity, some of compounds exhibits poor *in vivo* efficacy, which may attributed to high Clog P values. The SAR of diphenyl ethers indicates that the dichloro substitutions on ring-B of TCl can be attributed for the higher log P values. The studies also indicated the compounds were to be involved in unfavorable steric interactions with the enzyme and the removal of chlorine functionality from the scaffold would increase the affinity of inhibitors by seven folds towards enzyme²⁰. Consequently, in the present investigation diphenyl ethers were designed with hydrophilic substitutions at the 4th position of ring-A and exclusion of chlorine substitutions on ring-B. The hydrophilic linkers were employed to achieve desired lipophilicity. The substitutions on aryl moiety with both electron donating and electron withdrawing functions were made towards experimenting and understanding the possible interaction to effect the inhibition of the enzyme²¹. Over all modifications of diphenyl ethers were aimed to reduce the inherent lipophilicity of TCl derivatives without compromising its orientations and catalytic interactions at the InhA binding site. The drug design strategy is depicted in **Figure-1**.

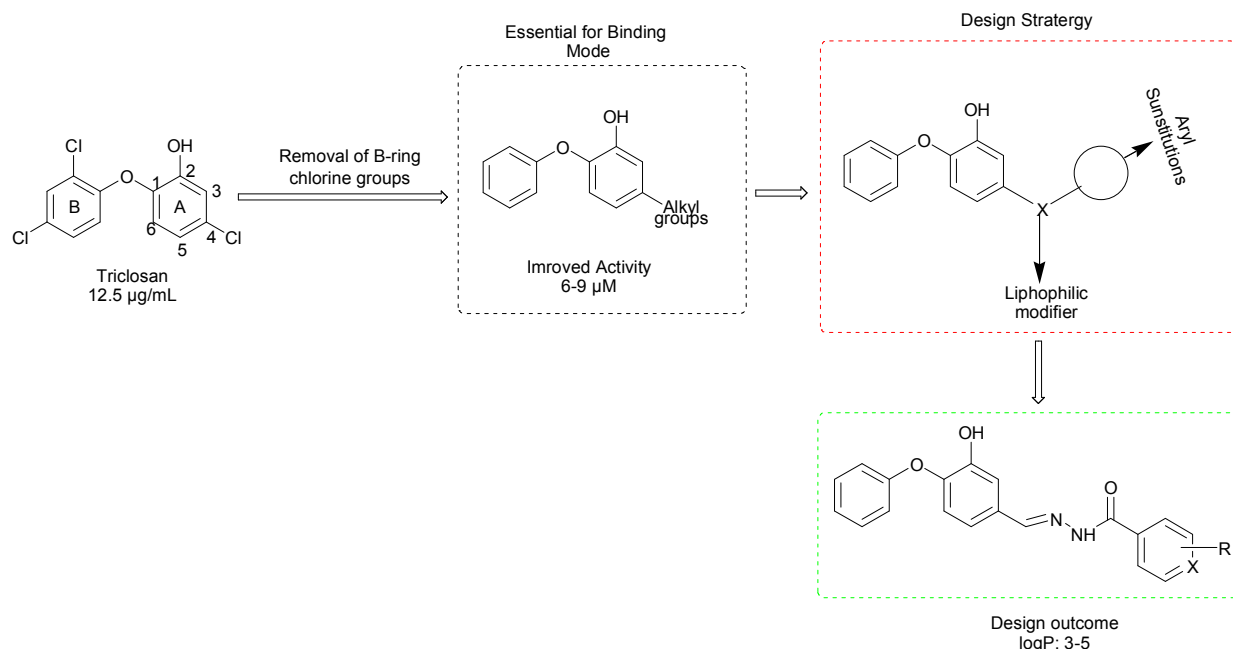


Figure-1: Design strategy of diphenyl ether analogues

2.2. Molecular modelling studies

2.2.1. *In silico* ADMET Studies

The designed compounds were screened for their appreciable ADMET properties using PreADME online tool²². All the compounds have appropriate values towards the evaluated *in silico* parameters. The Lipinski parameters of the molecules towards their biological efficacy were encouraging with zero Lipinski violation. The *in silico* ADMET results shows that the selected compounds have appreciable oral bioavailability and protein binding efficiency. The predicted oral availability was excellent as the molecules exhibited a calculated percentage of absorption (HIA) values ranging from 92 to 96%. The predicted plasma protein binding (PPB) exhibits parentage binding values ranging from 89 to 100 %. The compounds also shows moderate Caco2 cell permeability effect, which is in the range of 15-32 nm/sec. The compounds which have <2 blood brain barrier penetration values indicate poor penetration. The ADMET properties data is provided as supplementary material. Compounds that satisfied ADMET and Lipinski's parameters of drug likeness were docked against *Mtb* InhA.

2.2.2. Molecular docking study

The molecular docking technique was used to explore, predict and understand the protein/enzyme interactions with designed diphenyl ethers at *Mtb* InhA binding site. The docking study was performed on *Mtb* InhA pdb protein (PDB ID: 3FNG) using the SYBYL-X 2.1

molecular modelling software. The molecular docking study was executed initially by the analysis of binding site structural features, followed by docking and interpretation of the results and finally the validation of the docking protocol.

***Mtb* InhA binding site analysis:** The structural features of InhA reveals that it has four monomer units and each consists of 269 amino acid residues. The molecular weight of each monomer unit is ~29000 Da. The monomer unit builds with Rossmann fold structure and the core of the binding site contains eight α helices and seven β sheets, representing the dinucleotide binding for the cofactor, NADH. The substrate binding loop is consisting of 15 amino acid residues (194–208) and further categorized into three regions, upper, middle and lower substrate binding loop (USL, MSL, and LSL) (**Figure 2**). The top USL cover the substrate binding pocket (SBP) by forming inter-loop interactions. The dinucleotide binding site is close to LSL and forms interactions with NADH.

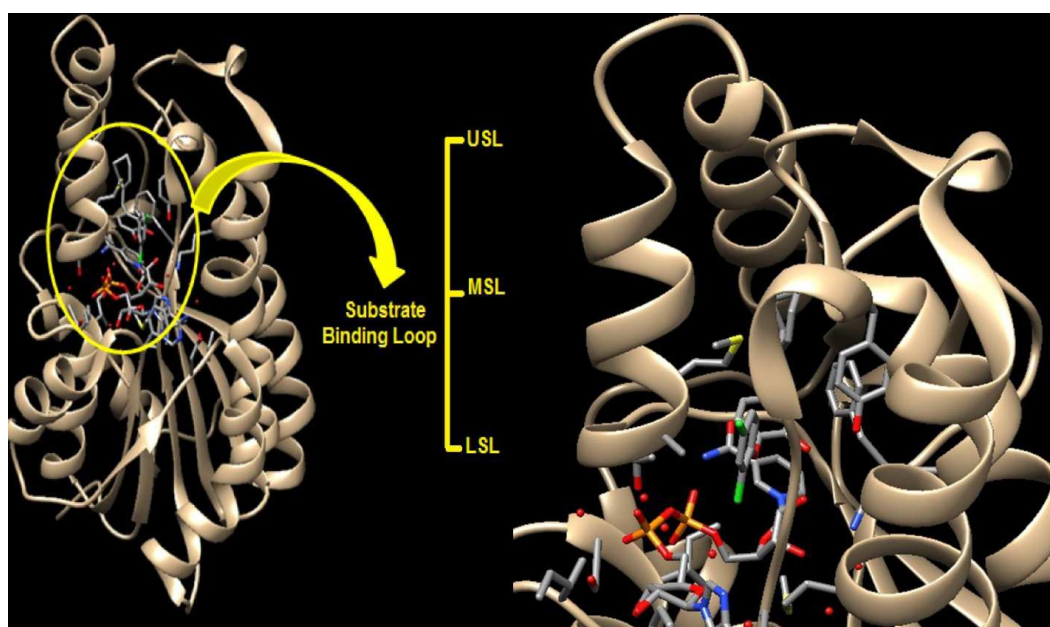


Figure-2: Substrate binding pocket of InhA and structural components. (USL: Upper substrate binding loop, MSL: Middle substrate binding loop and LSL: Lower substrate binding loop.)

The InhA complex of fatty acyl substrate and NAD⁺ cofactor crystal structure reveals that the fatty acyl substrate binds in U-shaped conformation. The residues Tyr158 and Lys165 are very much essential for the trans-enoyl reduction. They promote the removal of a proton from the 2'-nicotinamide -OH group. The InhA enzyme plays a crucial role in the reduction of C2–C3 double bond by transfer of hydrate ion to C3 carbon. The Tyr 158 hydroxyl group donates a

proton to the carbonyl oxygen of (C1) fatty acid results in an enolate anion. The substrate, fatty acyl chain is present in the core of lipophilic residues and most of the lipophilic residues are abreast to the SBL (Met103, Phe149, Tyr158, Lys165, Thr196, Met199, Leu207 and Ile215). The SBL of InhA is larger compared to enoyl-ACP reductases of other organisms and facilitates a deeper substrate binding area. The Tyr 158 interaction with fatty acyl substrate is the crucial feature in all of enoyl-ACP reductases

2.2.3. Docking Results:

Molecular docking results revealed that the basic scaffolds of **DE 1-10** (5-((Substituted imino)methyl)-2-phenoxyphenol) fits in the binding pocket of InhA similar to TCl and 5-(cyclohexylmethyl)-2-(2,4-dichlorophenoxy)phenol (co-crystallized ligand of 3FNG; JPL) (**Figure. 3a & 3b**). Furthermore, docking study reveal that the formation of hydrogen bonding interactions between phenolic –OH and ether oxygen of the designed compounds with Tyr-158 and NAD⁺ of *Mtb* InhA, which is vital as per the docking literature. The hydrogen bonding network is consistent in all the designed compounds, and this feature is reported to be a conserved one among all the InhA-inhibitor complexes including TCl. Hence, the core structural features of TCl (diphenyl ether nucleus) and the hydroxyl group in ring-A were kept intact in all the designed analogues. Based on docking scores (>7), interactions and binding with above said crucial residues; the best ranked molecules were considered for synthesis. The docking score data of the synthesized compounds is presented in **Table 1**.

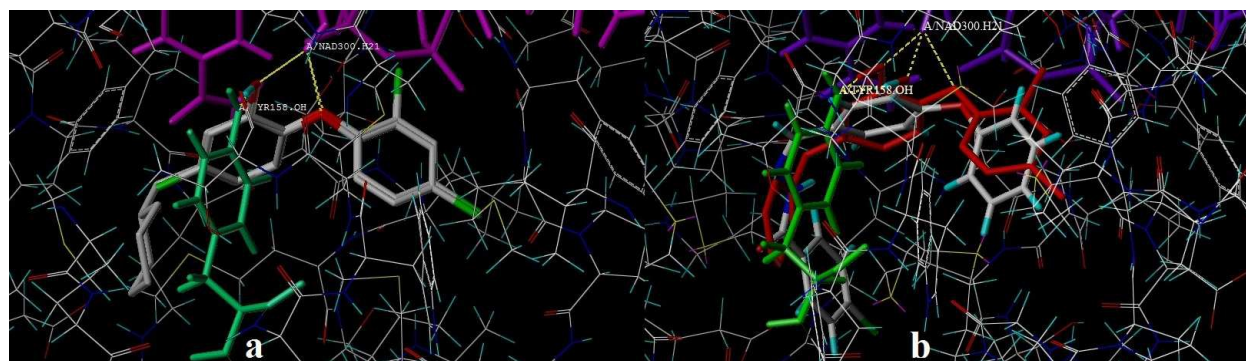


Figure-3: (a): Binding poses of TCl and JPL at InhA binding site, Green (TYR 158), Purple (NAD⁺), Yellow lines (Hydrogen Bonding). (b). Binding pose of compounds **DE3** and JPL at InhA binding site, Green (TYR 158), Purple (NAD⁺), Yellow lines (Hydrogen Bonding).

Table-1: Molecular docking scores of synthesized compounds **DE 1-10**.

Compounds	Docking scores		
	Total	Crash	Polar
DE1	7.74	-2.75	2.25
DE2	8.07	-3.15	2.11
DE3	7.06	-1.96	2.12
DE4	8.25	-1.44	1.02
DE5	8.56	-1.11	2.18
DE6	8.07	-1.02	1.13
DE7	8.71	-2.61	2.02
DE8	8.81	-1.58	2.21
DE9	8.04	-1.21	1.26
DE10	8.05	-2.08	1.84
JPL	8.86	-0.58	2.24
TCl	5.07	-0.29	2.41

Total Score = The total Surflex-Dock score expressed as $-\log(K_d)$.

Crash = The degree of inappropriate penetration by the ligand into the protein.

Polar = Contribution of the polar interactions to the total score.

2.2.4. Docking Validation:

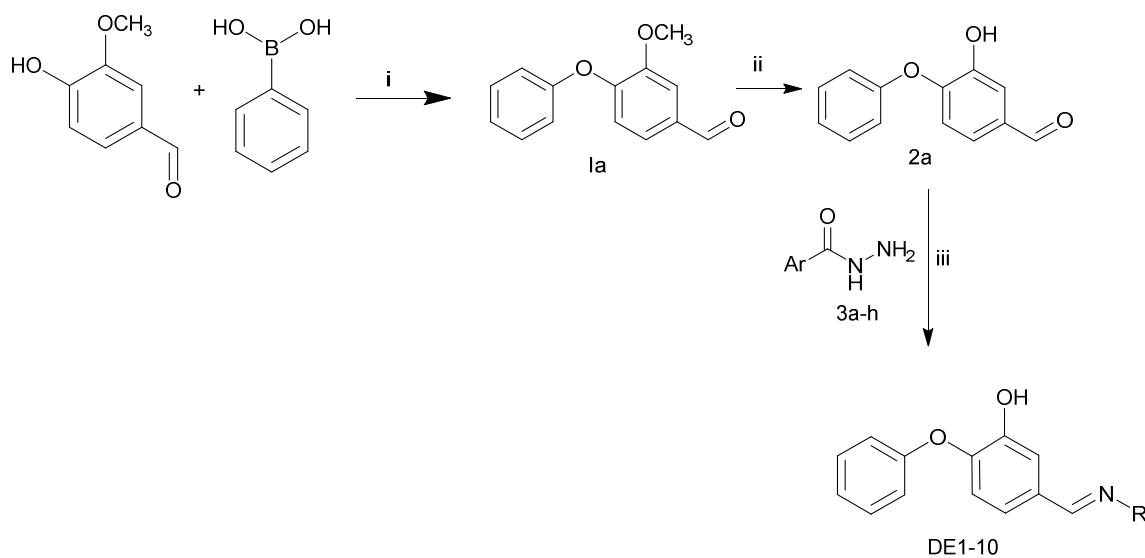
The accuracy of the docking protocol detailed under method was extensively validated by reproducing the ligand-receptor (*Mtb* InhA) complex (3FNG) deposited in the RCSB PDB. The Root Mean Square Deviation (RMSD) value and poses were used for validation of docking protocol. The co-crystallized ligand (JPL) of the PDB structure was extracted and docked along with the designed ligands. The docking poses of designed ligands were compared with the binding pose of JPL and TCl (**Figure-3a**). The RMSD value was calculated between the co-crystallized and docked ligand. The RMSD value for the co-crystallized and docked ligand was 0.948 Å and is lower than the acceptable limit (< 1.5 Å), accordingly indicates that the docking protocol is validated.

2.3. Chemistry:

The synthetic protocol for new series of diphenyl ether scaffold is outlined in **Scheme-1**. The starting material, 3-methoxy-4-phenoxybenzaldehyde (**1a**) was prepared according to Lam-Cham *O*-arylation with vanillin and phenyl boronic acid. Demethylation of methoxy aldehyde derivative **1** was carried out in the presence of Boron tribromide (BBr_3) at -78 °C (dry ice and acetone) to afford 3-hydroxy-4-phenoxybenzaldehyde (**2a**) which was further condensed with various acid hydrazides to afford title compounds **DE 1-10** (**Table-2**). The synthesized compounds were characterized by IR, ^1H NMR, ^{13}C NMR, mass spectral and elemental analysis data. In IR spectra, the absorption band around ~ 1590 cm^{-1} were observed in all the synthesized

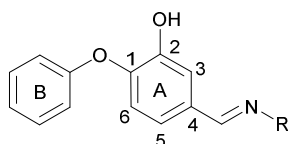
derivatives may be attributed for $-C=N$ stretching. The spectral characterization by ^1H NMR spectra of the derivatives indicates the chemical shift signals in the range of δ 6.6-7.9 ppm (Ar-H) as multiplet for aromatic protons. The NH proton of the amide group resonated as a singlet around δ 11.5 ppm attributing for the amide bond formation. Mass spectrum of the compounds exhibits molecular ion peak (M^+) corresponding to their respective molecular weights.

The ^1H NMR spectrum of the compound **1a** exhibited a singlet at δ 9.9 ppm value corresponds to aldehyde functionality and also exhibits 8 protons in the aromatic region (δ 7.6-7.0 ppm), it confirms the formation of diphenyl ether nucleus. In the ^1H NMR spectra of compound **1b**, the singlet at δ 10.1 and δ 9.9 ppm values were attributed to the proton of aldehyde functional group and the phenolic OH of diphenyl ether, respectively. The ^1H NMR spectral data concludes the formation of diphenyl ether and its demethylation product. The IR spectrum of **DE3** exhibited absorption bands at 3435 cm^{-1} attributing for N-H stretching and 1732 cm^{-1} accounting for stretching of C=O functionality. The ^1H NMR spectrum of the compound **DE3** exhibited singlet protons at δ 11.8 and 9.8 ppm values corresponding to NH of hydrazide functionality and phenolic OH group of diphenyl ether respectively. The spectral characterization data of all the synthesized compounds are in accordance with the proposed structures as depicted in the scheme. The experimental log P values of all the synthesized compounds were determined by RP-HPLC method to affirm and towards a comparative study with respect to the calculated log P values. The physicochemical properties data of **DE 1-10** is listed in **Table-2**.



Reagents and conditions : (i). $\text{Cu}(\text{OAc})_2$, $\text{C}_5\text{H}_5\text{N}$, CH_2Cl_2 , 25-27 $^\circ\text{C}$, 72 h. (ii). BBr_3 , CH_2Cl_2 , -78-10 $^\circ\text{C}$, 10 h. (iii). EtOH, reflux.

Scheme-1: Synthesis of designed compounds

**Table-2:** Physicochemical properties data of diphenyl ether derivatives.

Compound	R (A-ring C4)	Lipinski Rule of Parameters				log P (Experimental)
		Acceptor Count	Donor count	M.W.*	Clog P (Calculated)	
DE1		6	2	333.3	3.29	3.34
DE2		5	2	332.3	4.40	4.25
DE3		5	2	366.7	5.02	4.8
DE4		5	2	366.7	4.38	4.44
DE5		5	1	318.3	2.44	2.56
DE6		8	2	377.3	4.36	4.43
DE7		6	2	362.3	4.49	4.35
DE8		5	2	346.3	4.56	4.42
DE9		5	2	346.3	4.90	4.85
DE10		5	2	346.3	4.53	4.55

* Molecular Weight

2.4. Biological Activity:

2.4.1. Antitubercular Activity:

The synthesized compounds were evaluated for *in vitro* antitubercular activity by Microplate Alamar Blue assay (MABA) against *Mtb* H₃₇Rv strain. The antitubercular activities of **DE 1-10** are expressed as minimum inhibitory concentration (MIC) values using INH and TCl as the reference drugs towards a comparative study. The *in vitro* antitubercular evaluation of diphenyl ethers indicates that few of the tested compounds exhibit significant activity (**Table-3**). The compounds, **DE3** was found to be potent antitubercular among all tested compounds with a MIC value of 3.125 µg/mL. The results indicate that the better activity of compound **DE3** may be attributed to the electron withdrawing function chlorine at the *para* position and a comparatively higher log P value (4.8). In support of the above view, compound **DE2**, the phenyl derivative exhibited a MIC value of 6.25 µg/mL. Whilst, the methyl group substituted derivatives **DE8** and **DE9**, examples for electron donating groups were exhibiting a trivial antitubercular activity with MIC values >100 µg/mL. The *o*-chloro derivative (**DE4**) exhibited a higher MIC value (12.5 µg/mL) in comparison to the *p*-chlorophenyl derivative (**DE3**; MIC=3.125 µg/mL), but comparatively better than that of the *p*-nitrophenyl (**DE6** MIC=50 µg/mL). The better activity of compound **DE3** in comparison to **DE4** and **DE6** may be attributed to its log P value. The compound **DE3** log P value (4.80) is higher than that of compound **DE6** and **DE4**, which have log P value of 4.43 and 4.44, respectively. The efficiency of the drug to produce an antitubercular effect depends on the accumulation of the same in the cell and resulting in cell death. The higher lipophilic nature of compound **DE3** may be correlated to its potential to cross the phospholipid membrane of *Mtb* and leading to a significant accumulation of it in the cell and resulting in considerable antitubercular activity. The compounds with pyridinyl (**DE1** & **DE5**) substitutions demonstrated poor activity (MIC >100 µg/mL). The activity data reveals that the antitubercular activity of the derivatives drastically improved with the replacement of pyridinyl moiety (**DE1** and **DE5** MIC>100 µg/mL) by phenyl/ substituted phenyl moiety (**DE2**; MIC=6.25 µg/mL). Moreover, the low log P values of **DE1** (3.34) and **DE5** (2.56) may also be correlated with the lower antitubercular activity of pyridinyl derivatives. The investigation also indicated that the antitubercular activity decreases with increase in carbon chain length between the amide function and the phenyl moiety, compound **DE10**; benzyl derivative exhibited a MIC value of 12.5 µg/mL in contrast to **DE2** (MIC=6.25 µg/mL). The considerable antitubercular activity of

DE3 may be attributed to the electronegative functional group substitutions on the phenyl hydrazide moiety and a significantly higher log P (4-5) values.

The compounds exhibiting significant antitubercular activity (**DE2**, **DE3**, **DE4**, **DE7** and **DE10**) with a MIC values less than 25 $\mu\text{g/mL}$ were further screened for cell viability assay by Microculture Tetrazolium Assay (MTT) against Vero (epithelial cells) and HepG2 (hepatocytes) cell lines to ascertain their antitubercular activity is not due to cytotoxicity and also to highlight their safety profile on normal cell. The approximate CC_{50} values and selectivity index (SI) are tabulated in **Table 3**. These findings indicate that the active derivatives target *Mtb* to a greater extent compared to macrophage cell lines.

Table-3: *In vitro* antitubercular, antibacterial activity (MIC) and cytotoxicity (CC_{50}) of diphenyl ether derivatives

Compounds	MIC ^a ($\mu\text{g/mL}$)			CC ₅₀ ^b ($\mu\text{g/mL}$)		SI ^c
	<i>Mtb</i> H ₃₇ R _v	<i>S.aureas</i>	<i>E.coli</i>	Vero	HepG2	
DE1	>100	6.25	12.5	nc	nc	-
DE2	6.25	3.125	3.125	>300	>300	>10
DE3	3.125	3.125	6.25	>300	>300	>10
DE4	12.5	3.125	12.5	>300	>300	>10
DE5	>100	25	12.5	nc	nc	-
DE6	50	12.5	25	nc	nc	-
DE7	25	12.5	50	>300	>300	>10
DE8	>100	25	12.5	nc	nc	-
DE9	>100	25	100	nc	nc	-
DE10	12.5	12.5	25	>300	262	>10
INH	<3.125	-	-	nc	nc	-
TCI	12.5	-	-	nc	nc	-
Ampicillin	-	<3.125	<3.25	nc	nc	-

nc: not carried out

^a MIC = minimal drug concentration required to stop the growth of *Mycobacterium tuberculosis* H₃₇R_v.

^b CC₅₀ = minimal drug concentration required for 50% death of viable cells.

^c SI (Selective index) = CC₅₀/MIC.

2.4.2. Antibacterial Activity:

The synthesized compounds were also evaluated for *in vitro* antibacterial activity against Gram-positive *Staphylococcus aureus* (ATCC-25923) and Gram-negative *Escherichia coli* (ATCC-25922) by tube dilution method. The antibacterial data (**Table 3**) reveals that few of the diphenyl ether derivatives exhibited significant activity against the tested strains. Among the tested, compounds **DE2**, **DE3** and **DE4** have shown potential antibacterial activity with a MIC value of

3.125 $\mu\text{g/mL}$ against *S.aureus*. While, compound **DE3** was also effective against the *E.coli* with a MIC value of 6.25 $\mu\text{g/mL}$.

2.5. Molecular dynamic studies

The synthesized compounds were subjected to molecular dynamics (MD) simulation studies in comparison to the well-known inhibitor, **TCI** and **JPL** (3FNG co-crystallized ligand). The MD trajectories from the end of the simulation time were used to apply the MM-PB/SA method. The absolute free energy of a system is estimated from a combination of molecular mechanics following the Poisson–Boltzmann protocol. This protocol involves the estimation of electrostatic free energy determined from the exposed surface area and estimate of entropy of the system derived from normal mode calculations. RMSD plots of the simulation studies are presented in **Figure-4**. The RMSD plot shows that all the molecular dynamic simulation systems were stabilized and the results highlighting that designed ligands are stable in InhA core. The MM-PB/SA results and the average of the RMSD values (0-5 ns) for all the evaluated molecules are presented in **Table 4**. The studies indicate that few of the compounds have shown better binding free energy ($\Delta G_{\text{binding}} > -29$) than that of the **TCI** ($\Delta G_{\text{binding}} = -14.70$) and **JPL** ($\Delta G_{\text{binding}} = -28.96$). The results highlight that the best active compounds would have a better inhibitory efficacy than **TCI** and comparable to that of **JPL** at *Mtb* InhA binding site. The video files of molecular dynamic trajectories and detailed report files of MM-PB/SA are given as supplementary data.

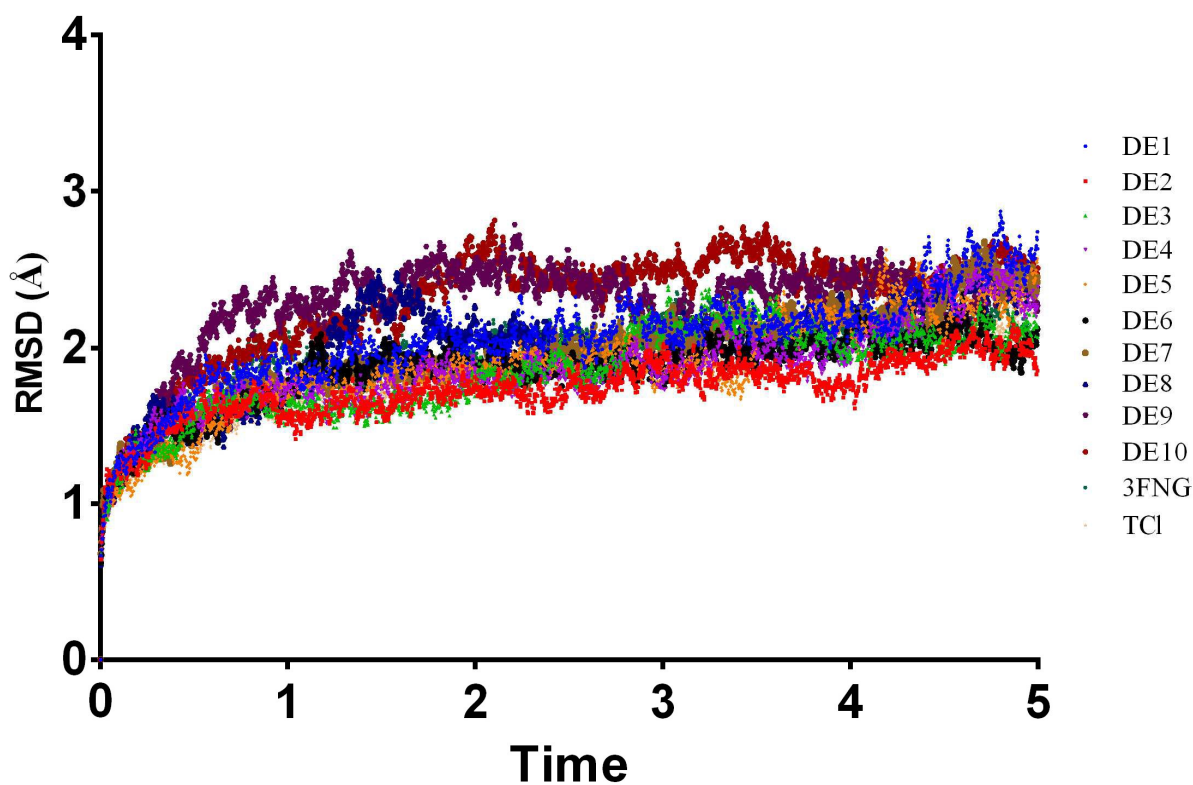


Figure-4: MD simulations RMSD plots of TCl (green), JPL (blue) and DE3 (red).

Table-4: Calculated MMPBSA binding free energies of the compound DE3, TCl and JPL

Cpd Code	Avg. RMSD (Å)	MM-PB/SA Results			
		ΔE_{VDW}	ΔE_{EL}	ΔE_{PB}	ΔG
DE1	2.05	-49.73	-20.08	49.03	-21.25
DE2	1.73	-49.80	-11.39	39.96	-25.46
DE3	1.84	-54.54	-35.90	65.15	-29.56
DE4	1.86	-49.24	-9.26	36.86	-26.04
DE5	1.88	-43.39	-7.95	34.66	-20.73
DE6	1.85	-44.09	-27.89	43.91	-24.29
DE7	1.95	-49.28	-15.84	41.70	-28.01
DE8	2.01	-40.12	-16.45	45.14	-22.62
DE9	2.26	-47.13	-5.14	36.35	-20.49
DE10	2.29	-54.26	-22.06	51.43	-29.34
TCl	1.87	-36.41	-10.10	34.90	-14.70
JPL	1.96	-49.97	-3.36	28.69	-28.96

3. Conclusion

In the present investigation, a library of diphenyl ethers was designed by structure-based drug design approach. The ADMET studies indicate that designed compounds have drug-likeness properties. The docking study indicates that the best ranked diphenyl ether molecules exhibit major interactions with 2-hydroxyl moiety of the nicotinamide ribose and the hydroxyl group of Tyr158 residue at InhA, which are similar to TCI and JPL. Best ranked diphenyl ether derivatives were synthesized and evaluated for antitubercular and antibacterial activities. The antitubercular activity of tested compounds was encouraging. Wherein, compounds **DE2** and **DE3** were found to be the potent molecules with MIC value 3.125 and 6.25 $\mu\text{g/mL}$ respectively. The cytotoxicity results of the most active compounds indicate that the tested compounds are non-toxic. The selectivity index values were found to be >10 . The antibacterial activity of test compounds were promising and compound **DE3** was found to be an effective antibacterial agent against the tested bacterial strains. The molecular dynamics study supports that best active molecules have stable protein-ligand complex and exhibits better binding free energy.

4. Materials and Methods:

4.1. Molecular docking study

The 3D structures of the designed compounds were generated using SYBYL-X 2.1 molecular modelling software (Tripos Associates, St. Louis, MO, USA)²³. The molecules were subjected to energy minimization with MMFF94s force field using a distance dependent-dielectric function, energy gradient of 0.001 kcal/mol and electrostatics. The Surflex-Dock tool was used to dock the designed molecules against InhA binding site to identify the binding mode and structural optimization. Surflex-Dock adopted is an empirical scoring function and a patented searching engine was employed for molecular docking. The crystal structure of *Mtb* InhA complexed with 5-(cyclohexylmethyl)-2-(2,4-dichlorophenoxy)phenol (PDB ID: 3FNG, 1.97 Å X-ray resolution) was taken from the protein databank (<http://www.rcsb.org/pdb>)²⁴. The protein structure was prepared for the molecular docking study by removing all water molecules. The missing hydrogen atoms were assigned to the InhA crystal structure. The co-crystallized ligand (JPL) was extracted from the protein and used as reference molecule for the validation study. The protocol was generated by keeping the parameters of co-crystallized ligand (JPL), threshold and bloat parameters unchanged from the default values of 0.50 and 0 Å. The mode of interaction of the co-crystallized ligand against 3FNG (InhA crystal structure) was used as a standard docking

model. The molecular docking was performed by analyzing 20 poses per ligand without any constraints. The docked complex assumed to represent the protein-ligand interactions, which was selected based on docking score, the orientation of the ligands at the active site in a similar to reference ligands and preservation of the two key interactions (H- bonds with Tyr158 and NAD⁺).

4.2. Synthesis and Characterization of designed molecules

All the chemicals and solvents used in this study were procured from Aldrich Chemical Co., Spectrochem Ltd., and Sd fine chemicals. All commercially available reagents procured were used without further purification. Column chromatography was carried out on 100-200 mesh Silica Gel. The progress of the reactions was monitored by TLC using Aluminum backed sheets of Silica Gel-60 F24 (Merck). Melting points were recorded using laboratory melting point apparatus and are uncorrected. ¹H NMR spectra were recorded on a NMR Spectrometer (VNMRS400 - 400 MHz) using DMSO-*d*₆ as the solvent. Mass spectroscopy was performed using LC-MS using methanol as solvent. IR spectrum was obtained using FTIR Spectrophotometer (Shimadzu, Japan) using KBr pellets.

3-Methoxy-4-phenoxybenzaldehyde (1a)

To the stirred solution of vanillin (1 mmol) in anhydrous dichloromethane (60 mL), activated molecular sieves (4 Å, 2.5 g), phenylboronic acid (1.5 mmol), copper (II) acetate (1.5 mmol) and anhydrous pyridine (2 mmol) were added successively. The resulting suspension was stirred at 25–27 °C for 72 h²⁵. The progress of the reaction was monitored by TLC, using hexane:ethyl acetate (4:1) as the mobile phase. After the completion of reaction (72 h), the reaction mixture was diluted with dichloromethane and filtered under vacuum. The filtrate was washed with dilute aqueous hydrochloric acid solution (2M), followed by water, dried over anhydrous MgSO₄ and evaporated under vacuum. The crude compound obtained was purified by column chromatography over silica 100–200 with hexane:ethyl acetate (4:1) as the mobile phase to afford the target compound.

3-methoxy-4-phenoxybenzaldehyde (1a): Yield = 75%; mp = 40–42 °C; Anal.Calc. For C₁₄H₁₂O₃: C, 73.67; H, 5.30; Found: C, 73.62; H, 5.36 %; IR (KBr, ν_{\max} , cm⁻¹): 3051 (Ar-H), 2928 (C-H), 1674 (C=O), 1583, 1489, 1413 (Ar-C=C), 1276 (Asym. C-O-C), 1134 (Sym.C-O-C); ¹H NMR (400 MHz, DMSO-*d*₆): 9.94 (*s*, 1H, CHO), 7.62 (*s*, 1H, Ar-H), 7.54-7.56 (*d*, 1H,

Ar-H), 7.38-7.42 (*t*, 2H, Ar-H), 7.15-7.18 (*t*, 1H, Ar-H), 7.05-7.07 (*d*, 1H, Ar-H), 7.00-7.01 (*d*, 2H, Ar-H), 3.87 (*s*, 3H, CH₃); LC-MS (*m/z*): 229.2 [M⁺].

3-Hydroxy-4-phenoxybenzaldehyde (2a):

To the solution of compound **1a** (3 g, 13.16 mmol) in dichloromethane (50 mL), BBr₃ (1 mmol in dichloromethane 26.32 mmol) was added at -78 °C, and the reaction continued for 6 h at 0-10 °C. The progress of the reaction was monitored by TLC, using hexane:ethyl acetate (4:1) as mobile phase. The resulting reaction mixture was poured into water and extracted with ethyl acetate (3x50 mL). The organic layers were combined and washed with saturated the sodium bicarbonate solution, dried over anhydrous magnesium sulphate and evaporated under vacuum. The crude product obtained was purified by column chromatography over silica 100–200 with hexane:ethyl acetate (4:1) as the mobile phase to afford the target compound.

Yield = 55%; mp = 82–84 °C; Anal. Calcd. For C₁₃H₁₀O₃: C, 72.89; H, 4.71; Found: C, 72.92; H, 4.65 %; IR (KBr, ν_{max}, cm⁻¹): 3051 (Ar-H), 2928 (C-H), 1674 (C=O), 1583, 1489, 1413 (Ar-C=C), 1276 (Asym. C-O-C), 1134 (Sym.C-O-C); ¹H NMR (400 MHz, DMSO-*d*₆): 10.08 (*s*, 1H, CHO), 9.85 (*s*, 1H, OH), 7.54 (*d*, 1H, Ar-H), 7.42–7.32 (*m*, 3H, Ar-H), 7.32–7.20 (*m*, 1H, Ar-H), 7.20–7.07 (*m*, 2H, Ar-H), 6.86–6.84 (*d*, 1H, Ar-H).; LC-MS (*m/z*): 215.1 [M⁺].

Preparation of acid hydrazides : The acid hydrazides(**3a-h**) were prepared as per the reported procedure²⁶.

Synthesis of (*E*)-*N'*-(3-hydroxy-4-phenoxybenzylidene) isonicotinohydrazide (DE1):

To the solution of 3-Hydroxy-4-phenoxybenzaldehyde (1 mmol) in absolute ethanol (10 mL), Isoniazid (1 mmol) was added and refluxed for 4 h, allow the solution to cool it for 12 h. The progress of the reaction was monitored by TLC, using hexane:ethyl acetate (1:1) as a mobile phase. The reaction mixture was cooled, poured into water and the precipitate was filtered, dried. The crude compound obtained was purified by column chromatography over silica 100–200 with hexane:ethyl acetate (1:1) as the mobile phase to afford the target compound. Similar procedure was adopted to synthesize title compounds **DE2-10** using appropriate acid hydrazide.

(*E*)-*N'*-(3-hydroxy-4-phenoxybenzylidene)isonicotinohydrazide (DE1):

Yield = 75%; mp = 186–188 °C; Anal. Calcd. For C₁₉H₁₅N₃O₃: C, 68.46; H, 4.54; N, 12.61; Found: C, 68.41; H, 4.60; N, 12.58 %; IR (KBr, ν_{max}, cm⁻¹): 3556 (-OH), 3435 (-NH), 3055 (Ar, -CH), 1722 (-C=O), 1592 (C=N), 1221 (C-O-C); ¹H NMR (400 MHz, DMSO-*d*₆, δ ppm):

11.98 (*s*, 1H, CONH), 9.84 (*s*, 1H, OH), 8.77 (*s*, 2H, Ar-H), 8.35 (*s*, 1H, N=CH), 7.80-7.78 (*d*, 2H, Ar-H), 7.43-7.42 (*d*, 1H, Ar-H), 7.31-7.29 (*dd*, 2H, Ar-H), 7.12-6.88 (*m*, 5H, Ar-H); ^{13}C NMR (400 MHz, DMSO-*d*₆, δ ppm): 161.92, 157.74, 150.77, 149.88, 149.01, 145.49, 140.96, 131.40, 130.17, 122.98, 121.93, 121.73, 120.60, 117.32, 114.81; LC-MS (*m/z*): 334.14 [M^+].

(E)-N'-(3-hydroxy-4-phenoxybenzylidene)benzohydrazide (DE2): Yield: 68 %; mp = 118–120 °C (ethanol); Anal. Calcd. for $\text{C}_{20}\text{H}_{16}\text{N}_2\text{O}_3$: C, 72.28; H, 4.85; N, 8.43; O; Found: C, 72.30; H, 4.90; N, 8.40 %; IR (KBr, ν_{max} , cm^{-1}): 3565 (-OH), 3435 (-NH), 3058 (Ar, -CH), 1714 (-C=O), 1590 (C=N), 1228 (C–O–C); ^1H NMR (400 MHz, DMSO-*d*₆, δ ppm): 11.77 (*s*, 1H, CONH), 9.82 (*s*, 1H, OH), 8.35 (*s*, 1H, N=CH), 7.90-7.89 (*d*, 2H, Ar-H), 7.52–7.49 (*m*, 3H, Ar-H), 7.43-7.42 (*d*, 1H, Ar-H), 7.34–6.89 (*m*, 7H, Ar-H); ^{13}C NMR (400 MHz, DMSO-*d*₆, δ ppm): 163.47, 157.83, 149.89, 147.77, 145.26, 133.95, 132.12, 131.77, 130.14, 128.90, 128.02, 122.90, 121.79, 120.33, 117.24, 114.71, 114.71; LC-MS (*m/z*): 333.15 [M^+].

(E)-N'-(3-hydroxy-4-phenoxybenzylidene)-4-chlorobenzohydrazide (DE3): Yield: 70 %; mp = 154-156 °C (ethanol); Anal. Calcd. for $\text{C}_{20}\text{H}_{15}\text{ClN}_2\text{O}_3$: C, 65.49; H, 4.12; N, 7.64; Found: C, 65.55; H, 4.16; N, 7.66 %; IR (KBr, ν_{max} , cm^{-1}): 3564 (-OH), 3435 (-NH), 3056 (Ar, -CH), 1732 (-C=O), 1592 (C=N), 1230 (C–O–C); ^1H NMR (400 MHz, DMSO-*d*₆, δ ppm): 11.83 (*s*, 1H, CONH), 9.82 (*s*, 1H, OH), 8.34 (*s*, 1H, N=CH), 7.93-7.91 (*d*, 2H, Ar-H), 7.59-7.58 (*d*, 2H, Ar-H), 7.42 (*s*, 1H, Ar-H), 7.34-7.29 (*m*, 2H, Ar-H), 7.11–6.89 (*m*, 5H, Ar-H); ^{13}C NMR (400 MHz, DMSO-*d*₆, δ ppm): 162.39, 157.80, 149.88, 148.12, 145.37, 136.98, 132.64, 131.65, 130.38, 130.14, 129.96, 129.01, 122.92, 121.77, 120.40, 118.31, 117.26, 114.75; LC-MS (*m/z*): 367.11 [M^+].

(E)-N'-(3-hydroxy-4-phenoxybenzylidene)-2-chlorobenzohydrazide (DE4): Yield: 65 %; mp = 152-153 °C (ethanol); Anal. Calcd. For $\text{C}_{20}\text{H}_{15}\text{ClN}_2\text{O}_3$: C, 65.49; H, 4.12; N, 7.64; Found: C, 65.6; H, 4.10; N, 7.61; IR (KBr, ν_{max} , cm^{-1}): 3552 (-OH), 3425 (-NH), 3042 (Ar, -CH), 1734 (-C=O), 1594 (C=N), 1225 (C–O–C); ^1H NMR (400 MHz, DMSO-*d*₆, δ ppm): 11.87 (*s*, 1H, CONH), 9.84 (*s*, 1H, OH), 8.37 (*s*, 1H, N=CH), 7.94-7.89 (*d*, 2H, Ar-H), 7.59-7.58 (*d*, 2H, Ar-H), 7.44 (*s*, 1H, Ar-H), 7.41 (*s*, 1H, Ar-H), 7.36-7.34 (*d*, 1H, Ar-H), 7.13–6.92 (*m*, 5H, Ar-H); ^{13}C NMR (400 MHz, DMSO-*d*₆, δ ppm): 167.42, 159.78, 152.14, 149.82, 146.31, 139.26, 133.27, 131.93, 129.91, 129.64, 127.76, 126.41, 122.52, 119.73, 119.48, 117.39, 116.76; LC-MS (*m/z*): 367.11 [M^+].

(E)-N'-(3-hydroxy-4-phenoxybenzylidene)isonicotinamide (DE5): Yield: 54 %; mp = 135-136 °C (ethanol); Anal. Calcd. For C₁₉H₁₄N₂O₃: C, 71.69; H, 4.43; N, 8.80; Found: C, 71.70; H, 4.48; N, 8.76; %; IR (KBr, ν_{\max} , cm⁻¹): 3568 (-OH), 3048 (Ar, -CH), 1715 (-C=O), 1602 (C=N), 1216 (C-O-C); ¹H NMR (400 MHz, DMSO-*d*₆, δ ppm): 9.87 (*s*, 1H, OH), 8.64 (*s*, 2H, Ar-H), 8.37 (*s*, 1H, N=CH), 7.81-7.79 (*d*, 2H, Ar-H), 7.44-7.42 (*d*, 1H, Ar-H), 7.33-7.32 (*dd*, 2H, Ar-H), 7.08-6.82 (*m*, 5H, Ar-H); ¹³C NMR (400 MHz, DMSO-*d*₆, δ ppm): 167.92, 161.74, 154.77, 147.68, 147.14, 144.42, 141.16, 134.47, 130.87, 124.38, 123.23, 121.73, 121.61, 119.32, 114.81; LC-MS (*m/z*): 319.15 [M⁺].

(E)-N'-(3-hydroxy-4-phenoxybenzylidene)-4-nitrobenzohydrazide (DE6): Yield: 62 %; mp = 154-156 °C (ethanol); Anal. Calcd. For C₂₀H₁₅N₃O₅: C, 63.66; H, 4.01; N, 11.14; Found: C, 63.70; H, 4.15; N, 11.20 %; IR (KBr, ν_{\max} , cm⁻¹): 3560 (-OH), 3441 (-NH), 3065 (-CH), 1708 (-C=O), 1590 (C=N), 1225 (C-O-C); ¹H NMR (400 MHz, DMSO-*d*₆, δ ppm): 12.04 (*s*, 1H, CONH), 9.83 (*s*, 1H, OH), 8.34-8.32 (*m*, 3H, N=CH and Ar-H), 8.14-8.12 (*d*, 2H, Ar-H), 7.45 (*s*, 1H, Ar-H), 7.34-7.30 (*m*, 2H, Ar-H), 7.13-6.89 (*m*, 5H, Ar-H); ¹³C NMR (400 MHz, DMSO-*d*₆, δ ppm): 162.39, 157.80, 149.88, 148.12, 145.37, 136.98, 132.64, 131.65, 130.38, 130.14, 129.96, 129.01, 122.92, 121.77, 120.40, 118.31, 117.26, 114.75; LC-MS (*m/z*): 378.5 [M⁺].

(E)-N'-(3-hydroxy-4-phenoxybenzylidene)-2-hydroxybenzohydrazide (DE7): Yield: 54 %; mp = 154-156 °C (ethanol); Anal. Calcd. For C₂₀H₁₆N₂O₄: C, 68.96; H, 4.63; N, 8.04; Found: C, 68.90; H, 4.68; N, 8.07 %; IR (KBr, ν_{\max} , cm⁻¹): 3563 (-OH), 3430 (-NH), 3058 (-CH), 1726 (-C=O), 1590 (C=N), 1225 (C-O-C); ¹H NMR (400 MHz, DMSO-*d*₆, δ ppm): 11.88 (*s*, 1H, CONH), 11.79 (*s*, 1H, OH), 9.85 (*s*, 1H, OH), 8.37 (*s*, 1H, N=CH), 7.89-7.87 (*d*, 1H, Ar-H), 7.45-7.40 (*d*, 2H, Ar-H), 7.33-7.29 (*m*, 2H, Ar-H), 7.13-7.02 (*m*, 2H, Ar-H), 6.98-6.89 (*m*, 5H, Ar-H); ¹³C NMR (400 MHz, DMSO-*d*₆, δ ppm): 165.22, 159.59, 157.77, 149.89, 148.76, 145.51, 134.26, 131.50, 130.16, 128.91, 122.95, 121.74, 120.56, 119.38, 117.74, 117.30, 116.26, 114.87; LC-MS (*m/z*): 349.13 [M⁺].

(E)-N'-(3-hydroxy-4-phenoxybenzylidene)-4-methylbenzohydrazide (DE8): Yield: 60 %; mp = 150-151 °C (ethanol); Anal. Calcd. For C₂₁H₁₈N₂O₃: C, 72.82; H, 5.24; N, 8.09; Found: C, 72.85; H, 5.19; N, 8.12 %; IR (KBr, ν_{\max} , cm⁻¹): 3558 (-OH), 3438 (-NH), 3051 (Ar, -CH), 1728 (-C=O), 1585 (C=N), 1238 (C-O-C); ¹H NMR (400 MHz, DMSO-*d*₆, δ ppm): 11.62 (*s*, 1H, CONH), 9.79 (*s*, 1H, OH), 8.34 (*s*, 1H, N=CH), 7.89-7.87 (*d*, 2H, Ar-H), 7.51-7.49 (*m*, 3H, Ar-H), 7.42 (*s*, 1H, Ar-H), 7.33-7.27 (*m*, 6H, Ar-H), 1.17 (*s*, 3H, CH₃); ¹³C NMR (400 MHz,

DMSO-*d*₆, δ ppm): 161.34, 158.11, 148.32, 146.27, 143.26, 131.96, 131.12, 129.77, 129.14, 127.92, 126.22, 121.96, 121.19, 119.73, 116.24, 114.21, 24.71; LC-MS (m/z): 347.2 [M⁺].

(E)-N'-(3-hydroxy-4-phenoxybenzylidene)-2-methylbenzohydrazide (DE9): Yield: 60 %; mp = 146-148 °C (ethanol); Anal. Calcd. For C₂₁H₁₈N₂O₃: C, 72.82; H, 5.24; N, 8.09; Found: C, 72.80; H, 5.22; N, 8.10 %; IR (KBr, ν_{\max} , cm⁻¹): 3562 (-OH), 3435 (-NH), 3048 (Ar, -CH), 1736 (-C=O), 1590 (C=N), 1233 (C-O-C); ¹H NMR (400 MHz, DMSO-*d*₆, δ ppm): 11.57 (s, 1H, CONH), 9.77 (s, 1H, OH), 8.35 (s, 1H, N=CH), 7.87-7.84 (d, 2H, Ar-H), 7.53-7.51 (m, 3H, Ar-H), 7.41 (s, 1H, Ar-H), 7.29-7.22 (m, 6H, Ar-H), 1.19 (s, 3H, CH₃); ¹³C NMR (400 MHz, DMSO-*d*₆, δ ppm): 163.11, 159.26, 148.12, 146.74, 144.16, 131.27, 130.82, 129.93, 128.74, 126.92, 126.31, 121.56, 119.84, 119.13, 117.44, 113.20, 22.64; LC-MS (m/z): 347.3 [M⁺].

N'-[(E)-(3-hydroxy-4-phenoxyphenyl)methylidene]-2-phenylacetohydrazide (DE10): Yield: 65 %; mp = 146-148 °C (ethanol); Anal. Calcd. For C₂₁H₁₈N₂O₃: C, 72.82; H, 5.24; N, 8.09; Found: C, 72.90; H, 5.20; N, 8.12 %; IR (KBr, ν_{\max} , cm⁻¹): 3556 (-OH), 3441 (-NH), 3052 (Ar, -CH), 1726 (-C=O), 1594 (C=N), 1236 (C-O-C); ¹H NMR (400 MHz, DMSO-*d*₆, δ ppm): 11.71 (s, 1H, CONH), 9.86 (s, 1H, OH), 8.33 (s, 1H, N=CH), 7.89-7.87 (d, 2H, Ar-H), 7.57-7.54 (m, 3H, Ar-H), 7.47 (s, 1H, Ar-H), 7.41-7.10 (m, 7H, Ar-H), 3.02 (s, 2H, CH₂C₆H₅); ¹³C NMR (400 MHz, DMSO-*d*₆, δ ppm): 162.64, 159.71, 149.22, 147.43, 144.26, 133.95, 132.12, 131.77, 130.14, 128.90, 128.02, 122.90, 121.79, 120.33, 117.24, 114.71, 114.71, 32.47; LC-MS (m/z): 347.4 [M⁺].

4.3. Antitubercular activity

Synthesized compounds were screened against *M. tuberculosis* H₃₇R_v using MABA^{27,28} and Middlebrook 7H9-S broth was used as media. Frozen stock culture suspension of *M. tuberculosis* H₃₇R_v (ATCC 27294) from Lowenstein-Jensen slants in complete 7H9 broth was vortexed, adjusted to a turbidity equivalent to that of a 1 McFarland standard (3x10⁸ CFU/mL). It was further diluted to a concentration of 2x10⁵ CFU/mL and used as inoculum in the MABA assay. Test samples and standard compounds (Isoniazid and TCl) were uniformly dissolved in DMSO and sterilized by filtering through syringe driven filters (0.22 μ m) to prepare stock solutions of concentration 20,000 μ g/mL. The stock solutions (4X) were diluted serially with media in a 96 deep well plate to afford working solutions. Dehydration of perimeter wells of the 96 well plates was prevented by filling with sterile deionized water during an incubation period. Twofold serial dilutions of the test compounds were done directly on the plate by using a multichannel

micropipette by adding Media (100 μL) was added to each well of the 96 well plate and 100 μL of inoculum (2×10^5 CFU/mL) was added to each well to obtain 200 μL and the final drug concentrations tests were 3.125–100 $\mu\text{g/mL}$. Isoniazid and TCI were used as standard and DMSO as blank. The error was minimized by applying positive control (inoculum) and negative control (media) in the plate. Then the plates were incubated at 37 $^\circ\text{C}$ under aeration. On the seventh day of incubation, 20 μL of Alamar blue reagent solution added to each well of the plate and incubated for another 24 h at 37 $^\circ\text{C}$. A change in color from blue to pink was considered as the growth of the Mycobacterium at that concentration of the drug. For better interpretation of the results, the color was compared to the color present in the growth control wells. The MIC was defined as the lowest concentration of drug that inhibited bacterial growth.

4.4. Cytotoxicity Screening

The cytotoxicity of the best active compounds was assessed by MTT²⁹ and against Vero and HepG2 cells (NCCS, Pune, India). The stock solutions of the test compounds were diluted in a 96 deep well plate aseptically with MEM (without FBS) to achieve concentrations 300, 250, 200, 150, 100 and 50 $\mu\text{g/mL}$. The 96 well plates containing the cells were taken and kept inverted on filter paper to remove the supernatant media and washed gently with PBS and decanted. 100 μL of sterile water were added to outer perimeter wells. Then 100 μL of each test compound dilutions were added to the wells. DMSO was used as a control and the plates were incubated in an incubator (5% CO_2) at 37 $^\circ\text{C}$ 72 h and 24 h for Vero cells and HepG2 respectively. After the incubation, plates were inverted on filter paper to remove the supernatant media followed by PBS washing. To this, 50 μL of MTT solution was added to each well in dark place and incubated for 3 h. After the incubation, the MTT solution was removed from the well by inverting gently on filter paper and 50 μL of DMSO was added to each well and kept in dark place for 2 h. Then the optical density readings of the plates were taken using Elisa reader at 540 nm. The safety profile (CC_{50}) was carried out by following equations 1&2.

Determination of safety profile (CC_{50})

$$\% \text{ Cell Viability} = \frac{\text{Optical Density of Test}}{\text{Optical Density of Control}} \times 100 \quad (1)$$

$$\text{Percentage cell Inhibition} = 100 - \% \text{ Cell Viability} \quad (2)$$

CC_{50} was calculated by extrapolating a graph with % cell inhibition on Y-axis against the concentration of test compound on X-axis.

4.5. Determination of log P

Reverse phase HPLC method was applied to determine the log P (lipophilicity) of the compounds^{30,31}. All the chromatographic runs were conducted on HPLC (Shimadzu, Japan) at room temperature using ODS-4 (Intersil ODS-4, 5 μ m, 4.6, 150 mm, GL Science Inc., Japan) column and PDA detector. Numerical analysis and data processing were done using Lab solution-2013 software. 3-Morpholinopropane-1-sulfonic acid (MOPS, 4.18 g) was added to 900 mL octanol saturated MilliQ water, and the volume was made up to 1 L. pH of the buffer was adjusted to 7.4. A mixture of methanol (0.25%v/v octanol) and buffer at the ratio of 60:40, 65:45 and 70:30, was used to elute the test sample. 5 μ L of the sample was injected, and the flow rate was kept at 1 mL/min. Signal was detected at λ_{max} 254 nm. Sample runtime was kept in between 20 min. Capacity factor (k_0) was calculated for each run by using the equation-3³².

$$k' = \frac{t_R - t_0}{t_0} \quad (3)$$

Where t_R is the retention time of the sample, t_0 is the retention time of blank (methanol). A graph was plotted by taking log k' (y-axis) and % methanol (3–4% concentrations) (x-axis). The logarithm of k' was extrapolated to a 0% concentration of methanol in the graph. log k' at 0% methanol was calculated from the regression equation ($R^2 = 0.99$) generated from the graph to determine log P of the compounds. The log P calculation of compound **DE-3** is given in the supplementary file.

4.6. Molecular dynamics

The molecular dynamic simulations were carried out by AmberTools 15.0 software. The topology and coordinate files were prepared for the selected *Mtb* InhA crystal structure complexes. The initial structure of the *Mtb* InhA-ligand complex was taken from the molecular docking study. The AMBER (Assisted Model Building with Energy Refinement) LeaP module^{33,34} was used to setup FF99SB force field parameters for protein and the ligand force fields parameters were taken from the General Amber Force Field (GAFF) and AM1 RSP atomic partial charges were assigned. The parameters missing for the NADH were taken from the amber parameter database, university of Manchester^{35,36}. The prepared complexes were solvated with TIP3P water model by creating an isometric water box, where the distance of the box was set to 10Å from a periphery of protein³⁷. Molecular complexes were neutralized through the AMBER tleap module by the addition of a necessary amount of counter ions (Na^+) to construct the system in electrostatically preferred positions. The whole assembly was then saved as per the

requirement of free energy calculation. This involved the preparation of parameter and coordinate files for the complex, protein and the ligand without salvation. Further, the prepared topology and coordinate files of solvated complexes were used as input for sander module of the AMBER³⁸. The optimization and relaxation of solvent and ions were performed by means of two energy minimization cycles using 1500 and 2000 steps. The initial 1500 steps of each minimization cycle were performed using steepest descent followed by conjugate gradient minimization for rest of the steps. In the first part of minimization, InhA-ligand complex was kept fixed to allow water and ion molecules to move, followed by the minimization of the whole system (water, ions and complex) in the second part. Heating was performed by six steps using a NVT ensemble for 500 ps where InhA-ligand complex was restrained with a very small force constant of 5kcal/mol/Å. The temperature was allowed to rise slowly in 0-300K in first 50 ps. Then the system was further equilibrated under constant pressure at 300K for the period of 200 ps without restraining on the complex. Final simulations (production phase) was performed for 5 ns on NPT ensemble at 300K temperature and 1atm pressure. The step size of 1fs was kept for the entire simulation study. Langevin thermostat and barostat were used for temperature and pressure coupling. SHAKE algorithm was applied to constrain all bonds containing hydrogen atoms. Trajectory snapshots were taken at each 2 ps of the production phase, which were used for final analysis. The minimization, equilibration and production were performed by sander module of Ambertools 15. The production run was considered for the analysis, which was carried out using the cpptraj module of the Ambertools 15³⁹ and Chimera⁴⁰.

4.6.1. MM-PB/SA Calculations

The MM-PBSA method⁴¹ was used to calculate the binding free energy of the protein-ligand complex. The binding free energy is estimated by the equation-4:

$$\Delta G = \Delta H - T\Delta S \quad (4)$$

T is the temperature of the system at 300 K. The binding free energy (ΔG) of the protein-ligand complex is computed as per equation-5.

$$\Delta G = G_{\text{complex}} - [G_{\text{protein}} + G_{\text{ligand}}] \quad (5)$$

Detailed calculations of MM-PB/SA were given in supplementary data file.

5. Acknowledgments

Authors are thankful to The Principal, JSS College of Pharmacy, JSS University, Mysuru, India for providing necessary facilities. Authors are beholden to DBT for the financial assistance (Ref. No: BT/PR5594/MED/29/540/2012). Authors express gratitude to The Director, University of Mysore, Central Instrumentation and Research Facility for spectral data.

Authors declare no conflict of interest

6. References

- 1 C. M. Lewandowski, N. Co-investigator and C. M. Lewandowski, *WHO Global tuberculosis report 2015*, 2015, vol. 1.
- 2 A. A. Velayati, P. Farnia and M. R. Masjedi, *Int. J. Clin. Exp. Med.*, 2013, **6**, 307–9.
- 3 K. Chung-Delgado, S. Guillen-Bravo, A. Revilla-Montag and Bernabe-Ortiz, *PLoS One*, 2015, **10**, e0119332.
- 4 B. C. Lafeuille E, Veziris N, Sougakoff W, Roure F, Le D₂ D, Dournon N, Caumes E, Jarlier V, Aubry A, Robert J, *Médecine Mal. Infect.*, 2016, **46**, 52–55.
- 5 T. J. Sullivan, J. J. Truglio, M. E. Boyne, P. Novichenok, X. Zhang, C. F. Stratton, H.-J. Li, T. Kaur, A. Amin, F. Johnson, R. A. Slayden, C. Kisker and P. J. Tonge, *ACS Chem. Biol.*, 2006, **1**, 43–53.
- 6 R. Rawat, A. Whitty and P. J. Tonge, *Proc. Natl. Acad. Sci. U. S. A.*, 2003, **100**, 13881–6.
- 7 N. Vale, P. Gomes and H. A. Santos, *Curr. Drug Metab.*, 2013, **14**, 151–8.
- 8 M. Seifert, D. Catanzaro, A. Catanzaro and Rodwell, *PLoS One*, 2015, **10**, e0119628.
- 9 G. P. Morlock, B. Metchock, D. Sikes, J. T. Crawford and R. C. Cooksey, *Antimicrob. Agents Chemother.*, 2003, **47**, 3799–805.
- 10 P. Kamsri, A. Punkvang, S. Hannongbua, P. Saparpakorn, P. Pungpo and Becerra, *RSC Adv.*, 2015, **5**, 52926–52937.
- 11 M. R. Kuo, H. R. Morbidoni, D. Alland, S. F. Sneddon, B. B. Gourlie, M. M. Staveski, M. Leonard, J. S. Gregory, A. D. Janjigian, C. Yee, J. M. Musser, B. Kreiswirth, H. Iwamoto, R. Perozzo, W. R. Jacobs, J. C. Sacchettini and D. A. Fidock, *J. Biol. Chem.*, 2003, **278**, 20851–9.
- 12 M. Chhibber, G. Kumar, P. Parasuraman, T. N. C. Ramya, N. Surolia and A. Surolia, *Bioorg. Med. Chem.*, 2006, **14**, 8086–8098.
- 13 J. S. Freundlich, F. Wang, C. Vilchèze, G. Gulten, R. Langley, G. A. Schiehser, D. P.

- Jacobus, W. R. Jacobs and J. C. Sacchettini, *ChemMedChem*, 2009, **4**, 241–8.
- 14 X. He, A. Alian, R. Stroud and P. R. Ortiz de Montellano, *J. Med. Chem.*, 2006, **49**, 6308–23.
- 15 X. He, A. Alian and P. R. Ortiz de Montellano, *Bioorg. Med. Chem.*, 2007, **15**, 6649–6658.
- 16 M. D. Wall, M. Oshin, G. A. C. Chung, T. Parkhouse, A. Gore, E. Herreros, B. Cox, K. Duncan, B. Evans, M. Everett and A. Mendoza, *Evaluation of N-(phenylmethyl)-4-[5-(phenylmethyl)-4,5,6,7-tetrahydro-1H-imidazo[4,5-c]pyridin-4-yl]benzamide inhibitors of Mycobacterium tuberculosis growth*, 2007, vol. 17.
- 17 U. H. Manjunatha, S. P. S Rao, R. R. Kondreddi, C. G. Noble, L. R. Camacho, B. H. Tan, S. H. Ng, P. S. Ng, N. L. Ma, S. B. Lakshminarayana, M. Herve, S. W. Barnes, W. Yu, K. Kuhen, F. Blasco, D. Beer, J. R. Walker, P. J. Tonge, R. Glynne, P. W. Smith and T. T. Diagana, *Sci. Transl. Med.*, 2015, **7**, 269ra3.
- 18 A. B. Dann and A. Hontela, *J. Appl. Toxicol.*, 2011, **31**, 285–311.
- 19 R. Petersen, *J. Nat. Sci.*, 2015, **73**, 389–400.
- 20 S. Sivaraman, T. J. Sullivan, F. Johnson, P. Novichenok, G. Cui, C. Simmerling and P. J. Tonge, *J. Med. Chem.*, 2004, **47**, 509–18.
- 21 H. Y. Jong, K. K. Chang, D. Yong, K. Lee, Y. Chong, M. K. Cheol, M. K. Jeong, S. Ro and M. C. Joong, *Antimicrob. Agents Chemother.*, 2007, **51**, 2591–2593.
- 22 K. T. N. S.K.Lee, I.H.Lee,H.J.Kim, G.S.Chang, J.E.Chung, in *EuroQSAR 2002 Designing Drugs and Crop Protectants: processes, problems and solutions*, , Blackwell Publishing, Massachusetts, USA., 2003, pp. 418–420.
- 23 I. Certara USA, *NJ 08540 USA*.
- 24 J. S. Freundlich, F. Wang, C. Vilchèze, G. Gulten, R. Langley, G. A. Schiehser, D. P. Jacobus, W. R. Jacobs and J. C. Sacchettini, *ChemMedChem*, 2009, **4**, 241–248.
- 25 T. A. Cinu, S. K. Sidhartha, B. Indira, B. G. Varadaraj, P. S. Vishnu and G. G. Shenoy, *Arab. J. Chem.*, 2015.
- 26 V. Judge, B. Narasimhan, M. Ahuja, D. Sriram, P. Yogeewari, E. De Clercq, C. Pannecouque and J. Balzarini, *Med. Chem. Res.*, 2012, **21**, 1451–1470.
- 27 B. Leonard, J. Coronel, M. Siedner, L. Grandjean, L. Caviedes, P. Navarro, R. H. Gilman and D. A. J. Moore, *J. Clin. Microbiol.*, 2008, **46**, 3526–3529.

- 28 C. Ryan, B. T. Nguyen and S. J. Sullivan, *J. Clin. Microbiol.*, 1995, **33**, 1720–1726.
- 29 K. Mohan Krishna, B. Inturi, G. V. Pujar, M. N. Purohit and G. S. Vijaykumar, *Eur. J. Med. Chem.*, 2014, **84**, 516–529.
- 30 S. Ong, H. Liu and C. Pidgeon, *J. Chromatogr. A*, 1996, **728**, 113–128.
- 31 S. K. Poole and C. F. Poole, *J. Chromatogr. B*, 2003, **797**, 3–19.
- 32 S. Gocan, G. Cimpan and J. Comer, *Adv. Chromatogr.*, 2006, **44**, 79–176.
- 33 V. Hornak, R. Abel, A. Okur, B. Strockbine, A. Roitberg and C. Simmerling, *Proteins*, 2006, **65**, 712–25.
- 34 V. Kumar and M. E. Sobhia, *PLoS One*, 2015, **10**, e0144635.
- 35 J. J. Pavelites, J. Gao, P. A. Bash and A. D. Mackerell, *J. Comput. Chem.*, 1997, **18**, 221–239.
- 36 † Ross C. Walker, ‡ Melanie M. de Souza, ‡ Ian P. Mercer, † and Ian R. Gould and ‡ David R. Klug*, 2002.
- 37 W. L. Jorgensen, J. Chandrasekhar, J. D. Madura, R. W. Impey and M. L. Klein, *J. Chem. Phys.*, 1983, **79**, 926.
- 38 D. A. Case, T. E. Cheatham, T. Darden, H. Gohlke, R. Luo, K. M. Merz, A. Onufriev, C. Simmerling, B. Wang and R. J. Woods, *J. Comput. Chem.*, 2005, **26**, 1668–88.
- 39 T. J. G. D.A. Case, J.T. Berryman, R.M. Betz, D.S. Cerutti, T.E. Cheatham, III, T.A. Darden, R.E. Duke, S. L. H. Gohlke, A.W. Goetz, N. Homeyer, S. Izadi, P. Janowski, J. Kaus, A. Kovalenko, T.S. Lee, I. P. Li, T. Luchko, R. Luo, B. Madej, K.M. Merz, G. Monard, P. Needham, H. Nguyen, H.T. Nguyen, J. S. Omelyan, A. Onufriev, D.R. Roe, A. Roitberg, R. Salomon-Ferrer, C.L. Simmerling, W. Smith and D. M. Y. and P. A. K. R.C. Walker, J. Wang, R.M. Wolf, X. Wu, in *AMBER 2015, University of California, San Francisco.*, University of California, San Francisco., 2015.
- 40 E. F. Pettersen, T. D. Goddard, C. C. Huang, G. S. Couch, D. M. Greenblatt, E. C. Meng and T. E. Ferrin, *J. Comput. Chem.*, 2004, **25**, 1605–1612.
- 41 I. Bill R. Miller, J. T. Dwight McGee, J. M. Swails, N. Homeyer, H. Gohlke and A. E. Roitberg, *J. Chem. Theory Comput.*, 2012, **8**, 3314–3321.